RADAR cooperative targets for wireless sensing: historical perspective and application to subsurface measurements

J.M Friedt[1,2], D. Rabus[3], G. Martin[1], F. Chérioux [1], M. Sato[2]
[1] FEMTO-ST Institute UMR 6174, 15B Avenue des Montboucons 25030 Besançon, France
[2] Center for Northeast Asian Studies, Tohoku University, 41 Kawauchi, Sendai 980-8576, Japan
[3] SENSeOR SAS, 15 Avenue des Montboucons 25030, Besançon, France

概要: acoustic wave transducers act as cooperative targets for passive, wireless sensing by converting an incoming electromagnetic pulse to an acoustic wave whose velocity is dependent, by design, with a given quantity under investigation. The acoustic wave is delayed and emitted back to the measurement electronics as an electromagnetic pulse by direct piezoelectric effect. In the context of sub-surface sensing, we address the challenges of diverting a classical geophysical instrument, a Ground Penetrating RADAR (GPR), for probing the cooperative target response. While the GPR provides both the electromagnetic pulse source and the means of recording the echo delays, representative of the acoustic velocity on the transducer and hence of the sensor environmental properties, the measurement range is dependent on the radiation pattern, emitted pulse spectra matching the transfer function of the target, and sensor antenna impedance matching properties. Furthermore, recovering the physical quantity under investigation assumes the timebase of the GPR to be more stable than the variation of the acoustic velocity induced by the environment of the sensor: we observe excessive timebase drift in the commercial GPR unit we use in experiments, and provide a solution by replacing an analog ramp generator with a stable, digital solution.
キーワード: Ground Penetrating RADAR, cooperative target, Surface Acoustic Wave

1. Introduction

Well before the advent of semiconductor based radiofrequency identification (RFID) tags for wireless radiofrequency communication between an active reader electronic system and a passive transducer, the idea of designing RADAR cooperative targets with varying properties was imagined from the experience acquired in monitoring reflected electromagnetic wave characteristics during the second world war [1]. Despite the commercial success of RFID devices, cooperative targets acting following linear energy conversion processes [2] exhibit several benefits, including always returning a signal however minute the incoming power – as opposed to a semiconductor system [3] which must be powered by a DC signal generated by the rectification of the incoming AC signal whose amplitude must exceed the diode threshold voltage – resistance to harsh environments and simple design as well as operating principles. Dielectric cooperative targets are plagued by large dimensions: delaying the signal returned by the target beyond clutter (Fig. 1) requires a dielectric delay line at least as long as the longest travel path of the electromagnetic wave, incompatible with compact sensors, with the option of virtually extending the dimensions of the transducer by multiplying the number of times the wave travels along the path (dielectric resonator approach). Notice that the information qualified here as clutter, or noise and artifacts in the returned signal that prevent detecting the echoes, is the same information that would be called interface reflections in classical GPR investigations. Furthermore, the sensing principle is restricted to varying intrinsic properties of the dielectric material the target is made of – dielectric dependence with temperature or moisture – frustrating the surrounding electromagnetic field or feeding the delay line with a varying load acting as the sensing element itself [4, 5, 6].

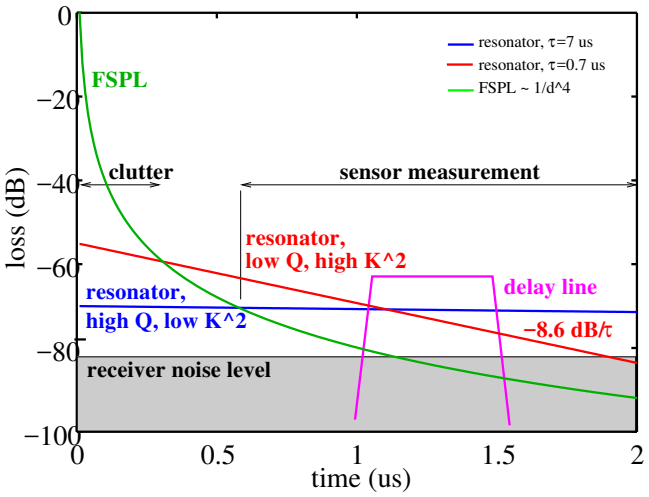

図 1: Returned signal power as a function of time: as clutter quickly fades out to reach power levels below the receiver noise level, the cooperative target must delay the returned signal long enough for the returned signal to be detectable above receiver noise level beyond clutter. Two strategies for delaying the signal are considered: delay line and resonator, and more specifically acoustic wave delay lines compatible with compact, robust sensor applications.

Since the early days of analog radiofrequency signal processing, the conversion of electromagnetic waves to the 10^5 times slower acoustic wave was identified as a means of shrinking the transducer dimensions. At

2017 年 11 月 30 日
東北大学　電気・情報系 103 会議室

300 MHz, a 1 m wavelength electromagnetic transducer is shrunk to a 10 μm wavelength acoustic transducer, meeting the compact sensor design requirements (Fig. 2). The detailed layout dimensions are given as inset in Fig. 4, while the electrode period was selected for a center frequency of 100 MHz : at 4000 m/s [7], such a frequency is achieved for a mechanical period of 4000/100 = 40 μm or an electrical period of the electrodes of 20 μm. Considering a 50% metalization ratio, the electrodes are 10 μm wide separated by 10 μm gaps, requiring cleanroom technology for fabrication. Furthermore, using a piezoelectric substrate for converting the electromagnetic to acoustic waves offers the opportunity of making the best out of the anisotropy of the substrate: varying the acoustic wave propagation direction allows for varying dependence of the acoustic velocity – and hence returned signal delay – with environmental conditions.

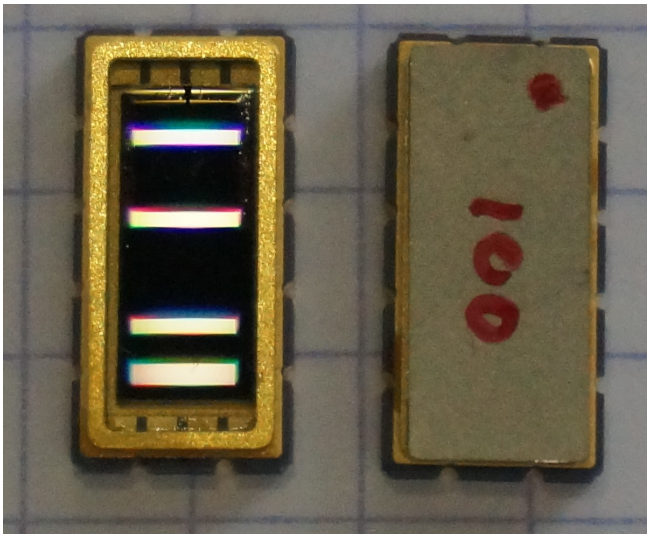

図 2: Packaged (left) and sealed (right) 100 MHz delay line made of black lithium niobate. The four light lines on the left device are reflections from the interdigitated electrode transducer (second from top) and acoustic reflectors (top and the two lines at the bottom). The grating lines on the paper used as background are separated by 5 mm.

Various characteristics of a cooperative target property can be investigated: radar cross section (i.e. returned magnitude), resonance frequency, echo time of flight, quality factor ... The former is a poor selection since excessively sensitive to the link budget and antenna impedance on both ends of the communication channel. Frequency, and its reciprocal time which is measured as a phase and hence the integral of the frequency, is the physical quantity measured with the highest accuracy and reproduced most easily with excellent references available in compact and low power formats. Selecting the measured quantity is not solely a matter of transducer design – both (wideband, high timing resolution) delay line and (narrowband, high frequency resolution) resonators are readily designed using classical acoustic transducer design techniques. Selecting the quantity under investigation and hence the sensor architecture is a matter of complete systems design, including interrogation system design, intended application conditions, possibly existing hardware, and not least compliance with regulations if commercial applications beyond the laboratory investigation are considered.

2. Historical background

Story has it that the emergence of the use of the signature of a signal backscattered by a target when illuminated by a RADAR seems to date back to the second world war * with German planes performing a barrel-roll when illuminated by RADAR to indicated friendly incoming aircrafts, consistent with the first publication dedicated to modulating on purpose the backscattered signal published in 1948 [1]. The intelligence community quickly accepted the approach and L. Theremin [8] developed The Thing for spying on the American embassador residence in Moscow [9]: a membrane vibrating under the pressure of sound varies the capacitance and hence the transfer function of a cavity resonator (Fig. 3). By illuminating the resonator with a continuous wave, an amplitude modulated signal is backscattered, carying the voice information: a tremendous achievement with the technology from the 1940s and 1950s (the microphone seems to have operated from 1945 to 1952). The British intelligence reversed engineered the device and developed its own passive microphone named SATYR [10].

Despite [1] being often heralded as the founder of RFID, the afore stated technologies differ fundamentally from the silicon-based impedance modulation by their linear interaction with the incoming radiofrequency power. Between the dedicated RFID and the passive linear cooperative target, the American NSA set of sensors [11] powered by the device under investigation (keyboard, video signal going from a computer to a screen) modulates the signal backscattered by the sensor when illuminated by a continuous wave. Development of passive cooperative targets interrogated by RADAR is hence a mature topic and widely available for the intelligence community, but its acceptance for industrial monitoring applications proves much more difficult, if only for the in-depth understanding of link budgets and radiofrequency

*Identification Friend or Foe, at `http://www.dean-boys.com/extras/iff/iffqa.html`, also cited by M.R. Rieback, B. Crispo & A.S. Tanenbaum, *The Evolution of RFID Security*, IEEE Pervasive Computing **5** (1), pp.62–69 (2006)

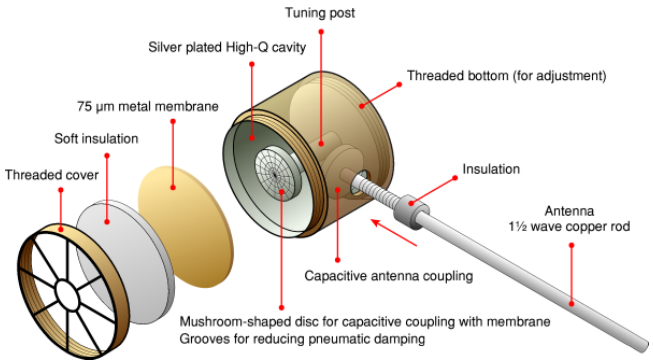

図 3: www.cryptomuseum.com/covert/bugs/thing/: figure depicting the operating principle of The Thing as a tunable resonator modulating the signal backscattered by the antenna when the membrane was set in motion by the pressure of a sound wave, varying the capacitance and hence the resonance frequency of the cavity.

communication basics hardly available from most heavy industry engineers. One population of users of radiofrequency signals well versed in the challenges of RADAR tuning has caught our attention: geophysicists using GPR.

3. Using a Ground Penetrating RADAR to probe acoustic transducers

Amongst the various electromagnetic pulse emitters – namely RADAR systems and of interest to us here the subset of Short Range RADAR systems [12] – available for non-military applications – are Ground Penetrating RADAR (GPR), widely used for geophysical shallow subsurface monitoring. Using GPR for probing acoustic transducers [13] meets two complementary requirements:

- usage case. Probing a transducer using a RADAR system, with a link budget decaying as the fourth power of the distance, requires some technical skill of the operator knowledgeable in the basics of antenna configurations and radiofrequency device tuning. If active sensors meet the requirements of the user, the link budget decaying as the square of the distance to the receiver is always more favorable than the RADAR link budget, and conditions in which active sensors are out of considerations are best addressed by passive sensors. Buried sensors meet such a requirement: since the civil engineering structures in which such passive sensors can be embedded, with expected life expectancies of several decades solely limited by the packaging of the sensor, cannot be met by compact, battery powered sensors. Obviously, opening a hole in a wall to replace a battery is not an option, nor is battery leakage in concrete once the energy source is exhausted.

- regulation compliance. GPR are included in the class of ultrawideband emitters (e.g. European Standard EN 302 066-1 and -2). While RFID has benefited from very favorable radiofrequency regulations with dedicated bands allowing for strong emitted power (125 kHz, 13.56 MHz, 868 MHz with maximum power reaching several watts), such bands do not meet the requirement of passive linear targets such as acoustic transducers, which must comply with existing regulations designed for different purposes. GPR allows for emitting strong pulses with a bandwidth compatible with typical delay line designs, and at low enough frequencies (50 to 800 MHz) to on the one hand penetrate deep in soil and concrete, while allowing for coarse optical cleanroom lithography with acoustic wavelengths of several micrometers.

Considering all these advantages in using GPR for probing acoustic transducers designed for acting as cooperative targets [14], what are the limitations of the approach ? We have identified two main limitations derived from using commercial, off the shelf GPR instruments beyond their intended usage: fixed wavelength rather than fixed frequency operation for most commercial GPR, and poor reference time-base insufficient with respect to the targeted accuracy.

All experiments are performed on reflective delay lines (Fig. 4) made of 200 nm platinum electrodes patterned over a thin chromium adhesion layer. The piezoelectric substrate is lithium niobate YXl/128°, selected for its strong electromechanical coupling and high temperature sensitivity, well suited for a temperature sensor. The SAW transducers, with electrode period tuned for the central operating frequency to be either 100 or 190 MHz, are packaged in radiofrequency compatible ceramic packages (Kyocera, Japan). The central frequencies have been selected for the SAW cooperative target to work best with 100 MHz unshielded antennas, 200 MHz unshielded antennas or 250 MHz shielded antennas, as provided by Malå Geoscience (now Guideline Geo, Malå, Sweden). All measurements are performed using the commercially available ProEx GPR control unit, provided by the same supplier. The custom control software available at sourceforge.net/projects/proexgprcontrol/ was used to collect all datasets.

Initial SAW delay line characterization is performed in the frequency domain using a network analyzer (Fig. 4, top), assessing whether the SAW transducer response matches the GPR emitted pulse spectra. Frequency

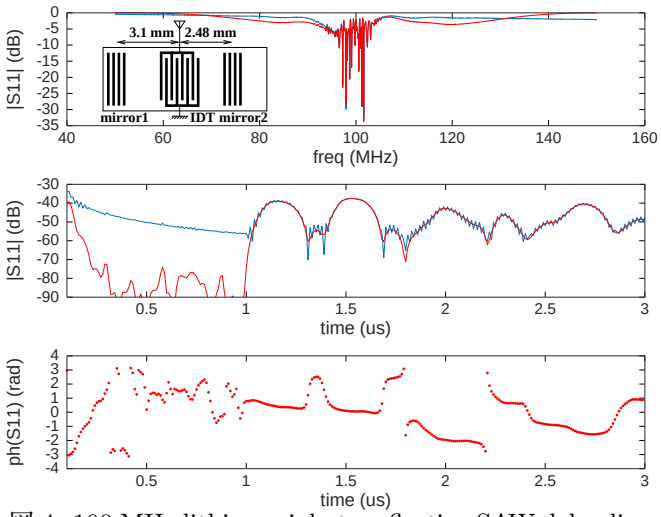

図 4: 100 MHz lithium niobate reflective SAW delay line transfer function, in the frequency domain (top) and the time domain (middle and bottom, magnitude and phase respectively) as found by inverse Fourier transform of the former. Windowing (red – Blackman window) helps lowering the baseline level with no effect on the insertion losses or the phase observed in the time domain. Inset: geometry of the delay line, defining the schematic position of the interdigitated transducer (IDT) between the two mirrors patterned on the piezoelectric substrate.

to time domain processing is needed to assess the expected GPR response, with echos delayed by durations defined by the interdigitated transducer (IDT) to mirror distance d and the acoustic velocity v. Since the distance is fixed and the velocity is dependent on the SAW transducer environment, the delay $\tau = d/v$ is representative of the physical quantity under investigation. Two echoes induced by two mirrors patterned on both sides of the IDT are visible in Fig. 4 (middle and schematic in the top inset), with delays of about 1.25 and 1.55 μs, as defined by distances d of 2480 and 3100 μm respectively, consistent with the Rayleigh wave tabulated velocity of 3979 m/s [15] on lithium niobate YXl/128°. The electromechanical coefficient $K^2 = 2\frac{\Delta v}{v} = 5.4\%$, with Δv the metalized to free surface acoustic wave velocity difference, hints at insertion losses of $20\log_{10}(K^2) = -25$ dB: the higher losses (-40 dB) seen in Fig. 4 (middle) are due to the excessive bandwidth of the measurement on the network analyzer whose frequency span was widened to clearly show the acoustic bandwidth of the device. The measurement bandwidth on Fig. 4 (right) was adjusted to optimize returned power by matching the probe signal bandwidth with the SAW reflective delay line bandwidth. The time delay of the echoes is accurately measured as a phase $\varphi = 2\pi d/\lambda$ with λ the acoustic wavelength, as seen on Fig. 4 (bottom). Keep in mind when converting from the frequency domain to the time domain (Fig. 4, middle and bottom) when using numerical processing software such as Matlab or GNU/Octave that their convention of positioning the 0-frequency differs from the one expected from radiofrequency signal processing: in the former software, the 0-frequency is located on the left part of the chart and the sampling frequency on the right part of the chart. Radiofrequency signal processing and demodulation expect the 0-frequency to lie in the middle of the chart, with minus half the sampling frequency and half the sampling frequency lying on the left and right part of the chart respectively. Converting the frequency measurement obtained on a network analyzer to the time domain requires converting from one convention to the other, as conveniently provided by the `fftshift()` function of these processing software. The magnitude of the time-domain response is not affected by this convention issue, but the phase is erroneous if the center frequency is not brought to the center of the chart during the conversion from frequency to time domain.

Throughout this document, time delay through phase measurement is performed in a differential approach to get rid of the additional delay depending on the RADAR to target distance: subtracting the phase of two echoes eliminates the common time of flight term and is representative solely of the acoustic velocity. As is classically known in RADAR signal processing, the matched filter is the cross-correlation: in our case, the incoming electromagnetic pulse, converted to an acoustic wave through the inverse piezoelectric effect of the substrate, is reflected twice by two mirrors located at different distances from the IDT. These two echoes are converted back to an electromagnetic wave by direct piezoelectric effect and detected by the RADAR. Cross-correlating the signals within the two time intervals in which the echoes are known to lie provides optimal noise rejection and signal identification. Furthermore, the cross correlation maximum position provides a fine estimate of the time delay between the two echoes: in all our processing steps, the cross-correlation maximum is detected, and fitted by a polynomial function for oversampling, assuming the cross-correlation maximum is locally symmetric and approximated at the second order by a parabola. The fine phase estimate is given by the parabola fit maximum, with a time-resolution improvement with respect to the sampling period equal to the signal to noise ratio. Hence, a core aspect of passive cooperative target with respect to RFID measurement is that the former is an analog measurement, with a measurement range that is not defined by reaching a threshold voltage to power a

digital circuit, but by a signal to noise ratio deteriorating the measurement quality until it becomes no longer usable.

The link budget is determined by the ability of the acoustic wave to propagate in the various media between the surface emitter and the sub-surface cooperative target, the electromechanical conversion efficiency, antenna impedance and transfer function matching to the incoming electromagnetic pulse, and returned signal losses through the same medium in which the electromagnetic wave propagates.

The link budget due to Free Space Propagation spreading of the electromagnetic power and conductivity losses in the medium are well documented and classically investigated when assessing GPR measurement range [16]. In the case of RADAR systems, with a target acting as a point like-source, the Free Space Propagation Loss (FSPL) rises as the distance to the fourth power since power spreads first on a sphere centered on the emitter, then reaches the target which itself acts as a source from which a new sphere defines the surface over which the minute returned power spreads again. The product of two power laws in which power spreads as the square of the distance yields a global loss law with distance appearing as the fourth power, an unfavorable condition with respect to powered sensors whose power law only decays as the square of the distance, justifying the use of cooperative targets in unique operating conditions where active sensors are not applicable. The electromechanical conversion, which replaces the RADAR cross-section of a target, is addressed by selecting strongly coupled piezoelectric substrates and acoustic wave modes meeting both the sensing capability and strong conversion efficiency: from a user perspective, an acoustic wave transducer is an electrical dipole returning a fraction of the incoming power, through a linear process (i.e. whatever the incoming power, some power will be returned). The last design issues we will discuss here lie in impedance matching and spectrum matching.

4. Fixed wavelength v.s fixed frequency

Most commercially available GPR emit a pulse by unloading a radiofrequency capacitor through an avalanche transistor. The broadband pulse is then filtered by the dipole antenna fitted on the avalanche transistor emitter: the transfer function of this dipole antenna, located on the ground surface for efficient coupling, is strongly influenced by the ground permittivity. The impact of the environment permittivity and conductivity on a dipole antenna property has been extensively investigated in [17] and will be further addressed below. Since the dipole length is fixed and the permittivity (and hence electromagnetic velocity) varies, the emitted central frequency varies accordingly, as does the impedance at resonance. However, the cooperative target is designed to operate at a fixed frequency range, determined by the spacing between interdigitated electrodes patterned on the piezoelectric substrate. The returned signal is the convolution of the incoming pulse with the impulse response of the acoustic transducer in the time domain, yielding an efficiency easier to grasp in the frequency domain as the product of the pulse spectrum with the acoustic wave transfer function. Any mismatch will prevent a fraction of the incoming electromagnetic pulse power to couple with the acoustic transducer and yield a loss in measurement range. Similarly, impedance mismatch prevents a fraction of the incoming electromagnetic pulse from being converted to an acoustic wave as it is reflected by the mismatched antenna. Ideal coupling conditions are met when the antenna impedance is the complex conjugate of the SAW impedance [18, 19]. Because the buried antenna impedance widely varies with surrounding permittivity, while again the acoustic transducer operates in a relatively narrow frequency band with respect to the ultrawideband GPR operating range, such a mismatch can become significant. A broadband antenna geometry, as found for example with a bowtie antenna classically used for GPR applications, will reduce the surrounding permittivity issue at the cost of poorer efficiency in the operating frequency band of the acoustic transducer.

5. Sensing example: sub-surface gas sensor

As a demonstration of sub-surface detection using a delay line, we illustrate the use of a lithium niobate delay line functionalized with a dedicated polymer layer tuned to spread homogeneously on the surface of a wafer by spin-coating, while including chemical functions able to selectively detect a gas under interest. In our case, the compound to be detected is hydrogen sulfide, a corrosive and deadly gas produced by bacteria as a consequence of oil well exploitation.

Fig. 5 exhibits a typical response of a polymer exposed to hydrogen sulfide, binding selectively lead ions (Pb^{2+}) trapped in the polymer matrix with the sulfur atom of the gas, making the initially hydrophobic polymer matrix hydrophilic. Upon exposure to water, the reaction consequence is enhanced by loading the polymer with water, inducing a significant mass loading observed as a strong variation of the acoustic velocity.

This measurements emphasizes the need for high stability time reference when using a Ground Penetrating RADAR for monitoring sub-surface sensors. Indeed, the targeted measurement is only a fraction of the period,

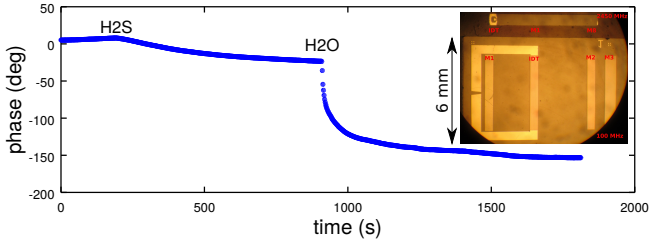

図 5: Sub-surface hydrogen sulfide detection using custom GPR – inset is a picture of the functionalized SAW delay line.

and any drift in the receiver time reference will overwhelm the measured signal. As an illustration of the implication of these considerations, using a 200 MHz sensor (5 ns period), a 150° phase rotation is equivalent to a 2 ns time delay in the sampling of an echo delayed by about 300 ns by the sensor. This 0.7% or or 7000 ppm is readily achieved with modern quartz-based time and frequency generation techniques, but is observed to be well below some of the commercial GPR implementations [20].

6. Dedicated sensor for buried concrete monitoring

Considering that the core function of the transducer acting as cooperative target is to separate clutter from the sensor response, we demonstrate here temperature monitoring in concrete with a dedicated sensor probed by a dedicated FSCW short range RADAR system operating in the European Industrial, Scientific and Medical (ISM) band centered on 433.92 MHz and 1.9 MHz wide (Fig. 6).

Initial curing of the concrete (Fig. 7) induces significant heating which is probed both by a reference Pt100 temperature sensor and by a SAW resonator. In addition to monitoring the resonance frequency – representative of the sensor temperature – the radiofrequency link budget quality is monitored since a feedback loop aims at controlling the emitted power in order to optimize the received power level. While the link budget is initially poor as the concrete is soaked with water, it quickly improves upon curing.

The sudden frequency variation 6 hour after the concrete was mixed and poured in a wooden mold (transparent to electromagnetic waves) is not explained but is attributed to stress induced in the sensor by the cured concrete acting on the rigid FR4 antennas. Despite this glitch emphasizing the need to decorelate stress and temperature, the general trend of temperature evolution is well observed. For a stress sensor, a temperature-compensated quartz cut would have been selected, reducing the temperature impact well below the stress impact on the sensing element.

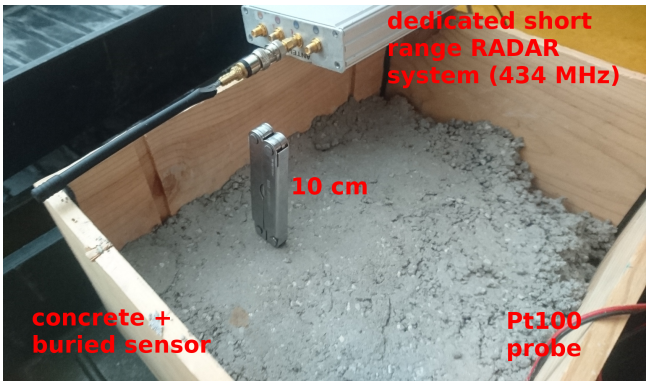

図 6: Experimental setup: a wooden mold is filled with 10 kg of concrete mixed with water and let to cure after inserting a 434 MHz sensor fitted to two 12 cm long FR4 dipole radiating elements and a Pt100 probe for reference. After the concrete was cured, the whole setup was inserted in a climatic chamber with the temperature raised to 160 °C before cooling back to room temperature.

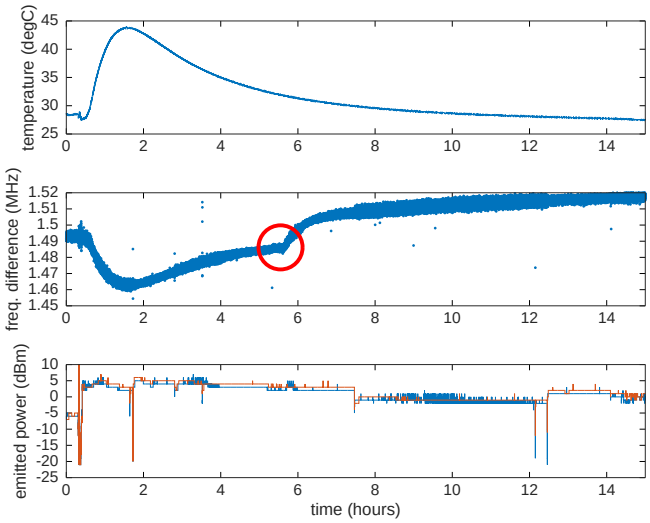

図 7: Concrete curing: the top chart reports on the Pt100 probe temperature measurement, the middle chart on the SAW sensor frequency difference representative of its temperature (middle), and the radiofrequency link budget (bottom). The latter chart spans from +10 dBm, when the maximum power is emitted by the short range RADAR system in a poor link budget configuration, and -21 dBm if saturation is reached.

Having cured the concrete block, we expose the brick in an oven to a 160 ° temperature, a level hardly achievable with battery powered autonomous sensors (Fig. 8). Here again, the SAW frequency behavior represents

closely the temperature evolution of the concrete as observed by the Pt100 probe, while the radiofrequency link budget remains about constant. In this example, the electromagnetic wave propagated a distance of about 15 cm between the short range RADAR and the concrete brick, and an additional 6 cm in concrete for the signal to reach the sensing element.

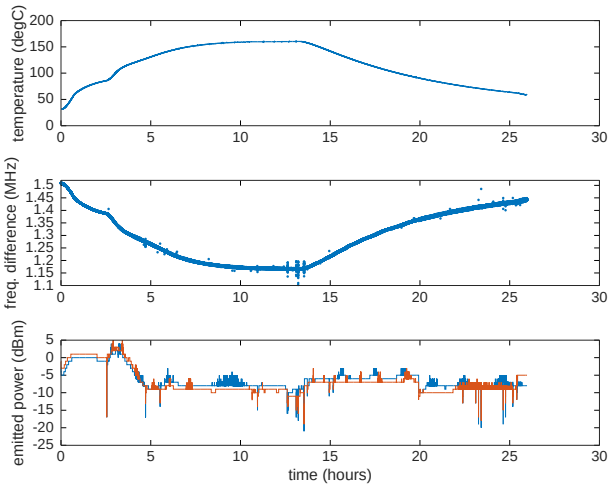

図 8: Second concrete curing experiment, with a set-point of 160 °C.

These two measurements are given as a demonstration of the ability of SAW sensors to meet demands of long term civil engineering structures monitoring, including when subject to earthquakes for assessing potential damages to buildings or bridges. The lack of local battery power guarantees that the lifetime of the sensing element is solely limited by the packaging resistance to the environment in concrete, and that the sensor is available when needed either for periodic inspection or assessment following natural catastrophic events.

7. Conclusion

Subsurface deployment of passive wireless sensors probed from the surface by using Ground Penetrating RADAR (GPR) provides a compelling scenario meeting user expectations and radiofrequency emission compliance. Knowing the limitations associated with the use of commercial GPR such as drift of the time base or limited time duration measurement, mitigation strategies include replacing the drifting analog timebase generator with a stable digital solution, and using a wideband antenna in addition to deploying sensors in environment with stable permittivity such as concrete so that the antenna operating frequency remains within the transducer passband. In all cases, tuning antenna dimensions for the pulse probe generated by the fixed-wavelength GPR to properly couple with the fixed-frequency sensor is a preliminary mandatory analysis prior to deployment.

We consider passive cooperative targets, and specifically SAW delay lines acting as sensors, as transducers well suited for the deployment in civil engineering structures, most probably made of concrete, for assessing the impact of natural disasters including earthquakes on the integrity of such structures. The impact of rebars on the measurement quality and range remains to be assessed in conditions representative of real environments, with the ability to adapt sensor operating frequency in the 100 to 2400 MHz range depending on allowed antenna dimensions, depth and rebar shielding frequencies.

Acknowledgement

J.-MF is grateful to the National University Corporation Tohoku University for granting an appointment as a 3-month visiting scientist to the Center for Northeast Asian Studies, aimed at promoting the use of cooperative GPR targets in civil engineering applications. This investigation is supported by SENSeOR SAS (France) and TOTAL SA (France) through grants supporting these research activities. The Ground Penetrating RADAR used in these investigations was acquired thanks to a Région Franche-Comté grant. The acoustic delay lines were manufactured in the cleanroom technological facilities MIMENTO of the FEMTO-ST Institute. The historical account was prompted by V. Plessky's (GVR Trade, Switzerland) description of the work of L. Theremin.

参考文献

[1] H. Stockman, "Communication by means of reflected power," *Proceedings of the IRE*, vol. 36, no. 10, pp. 1196–1204, 1948.

[2] J. Zhang, G. Y. Tian, A. M. Marindra, A. I. Sunny, and A. B. Zhao, "A review of passive RFID tag antenna-based sensors and systems for structural health monitoring applications," *Sensors*, vol. 17, no. 2, p. 265, 2017.

[3] S. Preradovic and N. C. Karmakar, "Chipless RFID: Bar code of the future," *IEEE microwave magazine*, vol. 11, no. 7, pp. 87–97, 2010.

[4] D. Thomson, D. Card, and G. Bridges, "RF cavity passive wireless sensors with time-domain gating-based interrogation for SHM of civil structures," *IEEE Sensors Journal*, vol. 9, no. 11, pp. 1430–1438, 2009.

[5] Y. Zhao, Y. Li, B. Pan, S.-H. Kim, Z. Liu, M. M. Tentzeris, J. Papapolymerou, and M. G. Allen, "Rf

evanescent-mode cavity resonator for passive wireless sensor applications," *Sensors and Actuators A: Physical*, vol. 161, no. 1, pp. 322–328, 2010.

[6] B. Kubina, M. Schusler, C. Mandel, A. Mehmood, and R. Jakoby, "Wireless high-temperature sensing with a chipless tag based on a dielectric resonator antenna," in *SENSORS, 2013 IEEE*. IEEE, 2013, pp. 1–4.

[7] J. J. Campbell and W. R. Jones, "A method for estimating optimal crystal cuts and propagation directions for excitation of piezoelectric surface waves," *IEEE Transactions on Sonics and Ultrasonics*, vol. 15, no. 4, pp. 209–217, 1968.

[8] A. Glinsky, *Theremin: Ether Music And Espionage*. University of Illinois Press, 2005.

[9] B. Fischer, "Leon theremin – cia nemesis. the soviet genius who spied for stalin," *declassified CIA document*, 2014, www.cia.gov/library/readingroom/docs/DOC_0006122432.pdf.

[10] P. Wright and P. Greengrass, *Spycatcher: The Candid Autobiography of a Senior Intelligence Officer*. Viking Press, 1987.

[11] J. Appelbaum, J. Horchert, and C. Stöcker, *Shopping for Spy Gear: Catalog Advertises NSA Toolbox*. Der Spiegel, 12/29/2013, leaksource.info/2013/12/30/nsas-ant-division-catalog-of-exploits-for-nearly-every-major-software-hardware-firmware/.

[12] G. L. Charvat, *Small and short-range radar systems*. CRC Press, 2014.

[13] C. T. Allen, K. Shi, and R. G. Plumb, "The use of ground-penetrating radar with a cooperative target," *IEEE transactions on geoscience and remote sensing*, vol. 36, no. 5, pp. 1821–1825, 1998.

[14] V. P. Plessky and L. M. Reindl, "Review on SAW RFID tags," *IEEE transactions on ultrasonics, ferroelectrics, and frequency control*, vol. 57, no. 3, 2010.

[15] D. Morgan, "Surface acoustic wave filters," *Amsterdam: Elsevier*, 2007.

[16] D. Daniels, "Ground penetrating radar (iee radar, sonar, navigation and avionics series)," *Stevenage, UK: Institution of Electrical Engineers*, 2004.

[17] R. King, "Antennas in material media near boundaries with application to communication and geophysical exploration, part i: The bare metal dipole," *IEEE transactions on antennas and propagation*, vol. 34, no. 4, pp. 483–489, 1986.

[18] K. Kurokawa, "Power waves and the scattering matrix," *IEEE transactions on microwave theory and techniques*, vol. 13, no. 2, pp. 194–202, 1965.

[19] C.-H. Loo, K. Elmahgoub, F. Yang, A. Z. Elsherbeni, D. Kajfez, A. A. Kishk, T. Elsherbeni, L. Ukkonen, L. Sydanheimo, M. Kivikoski *et al.*, "Chip impedance matching for UHF RFID tag antenna design," *Progress In Electromagnetics Research*, vol. 81, pp. 359–370, 2008.

[20] J.-M. Friedt, "Passive cooperative targets for subsurface physical and chemical measurements: a systems perspective," *IEEE Geoscience and Remote Sensing Letters*, vol. 14, no. 6, pp. 821–825, 2017.